

Correction: Comparison of Aerodynamic Characterization Methods for Design of Unmanned Aerial Vehicles

Author(s) Name: Moiz Vahora, Or. D. Dantsker

Author(s) Affiliations: Aero-Mechanical Engineer, M.S. Student, Department of Aerospace Engineering.

Correction DOI: 10.2514/6.2018-0272.c1

Correction Notice

Paragragh 1 on page 11 should be “K-epsilon ($k-\varepsilon$) turbulence model” not “K-epsilon ($k-\varepsilon$) turbulence mode”, there is no mode used in the simulations for turbulence just models.

Table 6 on page 15 has the XFLR5 and AVL results switch, which is fixed in this edit.

IV. High-Order Tool

A CFD simulation was performed using Ansys Fluent.³⁴ Using the CAD model described in Section II, a mesh was created using the Fluent meshing tool with 4 million cells, as shown in Fig. 13. The CFD simulation used a K-epsilon ($k-\epsilon$) turbulence model and was run on an 18-core Intel Xeon Processor E5-2697 v4 workstation with 32 GB DDR4 and a 4 GB GDDR5 NVIDIA Quadro K4200, which has 1344-CUDA cores. The freestream velocity of the analysis was 14 m/s, which operated under standard atmospheric conditions.

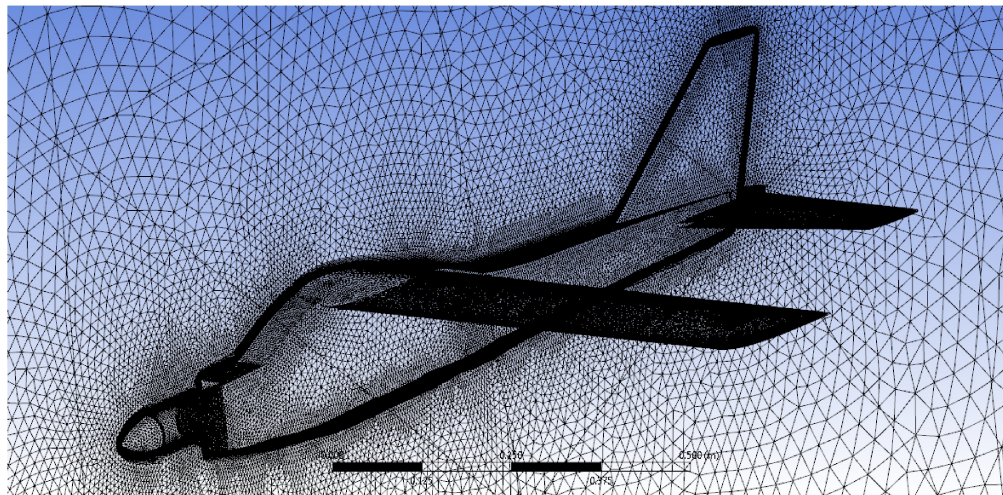


Figure 13. Avistar UAV CAD model meshed in Ansys Fluent with 4 million cells.

The analysis was conducted for angles-of-attack from -4 to 14 deg, with increments of 2 deg. Fig. 14 shows the lift and drag coefficients for each of the runs. Ansys Fluent predicted that aircraft stalls at approximately 10 to 12 deg and thus the stability derivatives were calculated using data from -4 to 8 deg, which appear linear. The stability derivatives are tabulated below.

$$\begin{array}{ll} C_{L\alpha} = 0.0667 & C_{L_0} = 0.3875 \\ C_{D\alpha} = 0.0067 & C_{D_0} = 0.05512 \\ C_{M\alpha} = -0.0340 & C_{M_0} = -0.00659 \end{array}$$

Streamlines for the wing, tail, and fuselage from the CFD analysis are shown in Figs. 15, 16, and 17, respectively. Warmer colors in the streamline figure indicate higher speeds while cooler colors show lower speeds. As seen, the flow is fully attached on the wing. At 4 deg, warmer shades of streamlines indicate higher flow acceleration compared to 10 and 14 deg. Beyond stall at 14 deg, flow separation was observed near the root while the flow is attached near the tip. This shows that the onset of stall begins near the hub region instead of the tip. Flow streamlines are attached on the tail until 10 deg but large separation can be observed for 14 deg. There is also a significant spanwise flow near the root of the horizontal tail at 14 deg. This is due the interference from the flow from the fuselage as shown below. Similarly, at lower angles-of-attack (4 deg), the flowfield is primarily two-dimensional on the fuselage. However, at higher angles-of-attack (14 deg) the flow becomes highly three-dimensional due to flow separation from the fuselage.

C. Results

During flight testing, the aircraft was flown through several low speed powered stalls in order to attempt to sweep the angle of attack of the aircraft. For this flight testing maneuver, the throttle was maintained above idle. The maneuver was performed by pitching the aircraft up to approximately 30 deg with the elevator, then all controls were centered, allowing the aircraft to transition through the partial stall. Due to the view point of the pilot on the ground, the aircraft entered the maneuver with a roll angle of around 35 degrees, which caused the aircraft to sideslip; the sideslip decreased as the dihedral leveled the aircraft off through the maneuver, though overshot. The motion of the recovery was recorded in order to provide a broad sweep of angles-of-attack at a relatively low rotation rate. State data of the recovery is presented in Fig. 18.

As the control surfaces were centered throughout the maneuver, the range of angles-of-attacks achieved were limited, specifically between -2 to 7 degs. In a similar manner, the total velocity the aircraft settled at throughout the maneuver was 16 m/s (36 mph). Fig. 19 shows the lift and drag coefficients from the maneuver. As mentioned in the previous section, the moment coefficient could not be calculated as the pitch moment of inertia data for the aircraft was not available at the time of paper submission. The stability derivatives of the lift and drag coefficients were calculated using data from -2 to 2 deg, which appear to be linear. The stability derivatives are tabulated as follows.

$$\begin{aligned} C_{L\alpha} &= 0.0606 & C_{L_0} &= 0.5345 \\ C_{D\alpha} &= 0.00237 & C_{D_0} &= 0.0489 \end{aligned}$$

VI. Results Comparison

The results from each of the analysis are tabulated in Table 6. The low order tools and CFD results predicted lift curve slope and zero angle-of-attack values within the same order of magnitude of the flight test and had similar trends. Ansys had the closest lift curve slope to the flight test, which may be attributed to 3D effects not accounted for in the low order tools, as XFLR5 and AVL had similar predictions. The drag predictions from AVL were lower than those from experimental data, XFLR5 and Ansys, which was attributed to how AVL does not include viscous effects. The drag predicted from Ansys Fluent is the closest to the flight test data results although the drag curve slope for XFLR5 and Ansys Fluent were lower than the experimental results by an order of magnitude.

Table 6. Aircraft characteristics and stability derivatives for each analysis run

	XFLR5	AVL	Ansys Fluent	Flight Test
$C_{L\alpha}$	0.0827	0.0810	0.0667	0.0606
$C_{D\alpha}$	0.0075	0.0043	0.0067	0.0237
$C_{M\alpha}$	-0.0249	-0.0193	-0.0340	—
C_{L_0}	0.357466	0.33088	0.3875	0.5345
C_{D_0}	0.020282	0.00633	0.05512	0.0489
C_{M_0}	-0.00799	-0.06364	-0.00659	—

The zero angle-of-attack moments predicted by XFLR5 and Ansys are very close though their slopes are within the same order of magnitude, whereas the moment predicted by AVL is greater than the previous solutions by an order of magnitude, which can also be attributed to viscous effects. The moment curve slopes from all three of the tools were within the same order of magnitude. The differences between the moment slopes could be attributed to viscous and 3D effects as the angle-of-attack increases, which will limit the the low order results to small angles-of-attack. The zero angle-of-attack moment from XFLR5 and Ansys are of the same order of magnitude, whereas the AVL results are greater by an order of magnitude. The difference in AVL moment results can be attributed to the lack of viscous effects in the calculations as drag contributes to the moment acting upon the aircraft.

As the aircraft was trimmed during the flight test, it was very difficult to accurately determine the zero angle-of-attack coefficients, especially as the trim values shifted. Although the zero angle-of-attack coefficients did not match the experimental results, the lift curve slopes computed from Ansys and the flight test were very close. As the zero lift coefficient derived from the flight test is higher than the CFD solution, the elevator control surfaces most likely were trimmed away from the center.